Ninth International Conference on Computational Fluid Dynamics (ICCFD9), Istanbul, Turkey, July 11-15, 2016

ICCFD9-2016-329

A Front Tracking Method for Computational Modeling of Temperature and Species Gradient Based Phase Change

Muhammad Irfan[1] & Metin Muradoglu[1]

[1] Department of Mechanical Engineering, Koc University, Istanbul 34450, Turkey

Corresponding author: mirfan13@ku.edu.tr

Abstract: A front tracking method is developed to simulate the liquid-gas phase change phenomenon during vaporization/evaporation process. One field formulation of the governing flow, energy and species equations are solved on an Eulerian grid with suitable jump conditions. Both phases are assumed to be incompressible; however, the divergence-free velocity field condition is modified to account for the phase change/mass transfer at the interface. Interface/front separates the phases and is composed of connected marker points that are tracked explicitly. Temperature gradient based phase change model calculates the heat source/sink at the interface by applying the energy conservation principle. For the species gradient driven phase change model, the Clausius-Clapeyron relation is used to find vapor mass fraction at the interface, which is subsequently used to find the mass flux and heat flux across interface. The implementation is validated against standard test cases such as 1D Stefan problem and the evaporation of a 2D static droplet. The non-dimensional evaporation mass flux across the interface is validated against an analytical model, assuming the interface temperature constant throughout the evaporation process. For a water droplet evaporating in air, the numerical results of wet bulb temperatures are compared with the psychrometric chart values and a good agreement is observed. Finally, 2D planar moving and deforming droplets are made to evaporate for different Eotvos (Eo) and Morton (Mo) Numbers. The implementation is grid convergent and mass is globally conserved for all the studied cases. The next step will be to incorporate chemical reactions into the present computational method using finite-rate chemical kinetic models.

Keywords: Front Tracking Method, Droplet Evaporation, Phase Change, Clausius-Clapeyron Relation.

1 Introduction

Various kinds of multiphase flows occur frequently in natural occurrences, industrial processes and biological systems. A moving rain droplet in air, a rising gas bubble in the water bed, gas bubbles release and movement in casting process, core annular flows for oil/gas transportation in petroleum industries, flows in pumps and turbines etc. are some of the practical examples. A better understanding of the physics of these interfacial flows is the key for the design improvement and system efficiency of systems involving such flows.

Direct Numerical Simulation has proved to be a powerful tool that helped designers to optimize design parameters to achieve excellent performance indicators. With the development of micro/nanoscale applications, the DNS has proved its importance since we can simulate the flows and processes that are almost impossible to study experimentally. Different forms of governing fluid flow equations are solved on suitable underlying grid depending on the geometric configuration. The main challenge in simulating interfacial flows is to accurately update the interface separating different fluids in the flow stream. Phase change process adds another dimension to multiphase flows. At the interface there is volume change associated with phase

change process. Evaporation and condensation are the two phase change phenomena that are very important from industrial applications point of view. Over the last two decades researchers have put efforts in this field to simulate the multiphase flows with phase change. Volume of fluid (VOF) [6, 12], level set [9, 14] and front tracking [4, 16] methods are the most common and well developed techniques to track or capture the fluid interface.

A front tracking method developed by Unverdi and Tryggvason uses one-field formulation of governing equations. The governing equations are solved on the fixed Eulerian grid whereas the interface is represented by connected marker points that are tracked explicitly. The detailed implementation of this method is discussed in [16, 15]. The method was first developed for buoyancy driven bubble. Juric and Tryggvason studied liquid-solid phase change phenomenon i.e., dentritic solidification [7], and the liquid-vapor phase change i.e., film boiling [8]. Esmaeeli and Tryggvason made improvements in the previous developed method for liquid-vapor phase change [1, 2].

In this paper, we present a front tracking method to simulate the liquid-vapor phase change owing to the temperature or the species concentration gradient at the interface. This phenomenon, called evaporation, occurs only at the surface. The governing flow, energy and species equations are solved on staggered marker-and-cell (MAC) grid. Source terms at the interface have been incorporated in the governing equations using delta functions or by the application of proper boundary conditions at the interface. For temperature gradient based phase change, heat flux at the interface is calculated by the application of energy conservation principle. For the species gradient based evaporation, the Clausius-Clapeyron equilibrium relation is applied to ultimately find the species mass fraction at the interface. Interface, separating two phases, is represented by connected marker points. The movement of front/interface marker points is contributed by both the local flow velocity and the heat flux component. First, the results are presented for temperature gradient based phase change model. The implementation is validated for 1D Stefan problem and the d^2-law for 2D static droplet case. The case of 2D gravity driven droplet is studied next for different Eotvos (Eo) and Morton (Mo) numbers. Next, we simulated the species concentration gradient based evaporation model. Non-dimensional evaporation mass flux is validated against a simplified analytical model. The results of 2D planar droplets moving under various flow conditions are presented next. The grid convergence and global mass conservation is demonstrated for the sample cases.

2 Mathematical Formulation

The one field formulation of the mass, momentum, energy and species conservation equations are expressed as

$$\nabla \cdot \mathbf{u} = \frac{1}{h_{lg}} \left(\frac{1}{\rho_g} - \frac{1}{\rho_l} \right) \int_A \delta(\mathbf{x} - \mathbf{x}_\Gamma) \dot{q_\Gamma} dA_\Gamma, \tag{1}$$

$$\frac{\partial \rho \mathbf{u}}{\partial t} + \nabla \cdot (\rho \mathbf{u}\mathbf{u}) = -\nabla p + \rho \mathbf{g} + \nabla \cdot \mu(\nabla \mathbf{u} + \nabla \mathbf{u}^T) + \int_A \sigma \kappa \mathbf{n} \delta(\mathbf{x} - \mathbf{x}_\Gamma) dA, \tag{2}$$

$$\frac{\partial T}{\partial t} + \mathbf{u} \cdot \nabla T = \frac{\nabla \cdot k \nabla T}{\rho c_p} - \frac{1}{\rho c_p} \left[1 - (c_{p,g} - c_{p,l}) \frac{T_{sat}}{h_{lg}} \right] \int_A \delta(\mathbf{x} - \mathbf{x}_\Gamma) \dot{q_\Gamma} dA_\Gamma, \tag{3}$$

$$\frac{\partial Y_\alpha}{\partial t} + \mathbf{u} \cdot \nabla Y_\alpha = \nabla \cdot D \nabla Y_\alpha + \frac{\dot{S_\alpha}}{\rho} \qquad \alpha = 1, 2, ..., n_s \, . \tag{4}$$

$\mathbf{u}$ is the velocity, h_{lg} is the latent heat of vaporization and $\dot{q_\Gamma}$ represents heat flux per unit time at the interface. Subscripts Γ, l and g represent the interface and the liquid and gas phases of a multiphase system, respectively. p is the pressure, and ρ and μ are the discontinuous density and viscosity fields, respectively. σ is the surface tension, κ is twice the mean curvature, and $\mathbf{n}$ is a unit vector normal to the interface. The surface tension acts only on the interface as indicated by the two-dimensional delta function δ whose arguments $\mathbf{x}$ and $\mathbf{x}_\Gamma$ are the point at which the equation is being evaluated and a point at the interface, respectively. T is the temperature, c_p is the specific heat at constant pressure and k is the thermal conductivity. Subscript *sat* denotes the saturation value of the variable. Y_α represents the mass fraction of species component α and D is the mass diffusion coefficient.

The energy and species jump conditions must be satisfied at the interface to ensure energy and mass conservation across the interface. These are

$$\dot{m_\Gamma} h_{lg} = \dot{q_\Gamma} = k_g \left.\frac{\partial T}{\partial n}\right|_g - k_l \left.\frac{\partial T}{\partial n}\right|_l, \tag{5}$$

$$\dot{m_\Gamma} Y_l^\Gamma - \dot{m_\Gamma} Y_g^\Gamma + \rho_g D \left.\frac{\partial Y}{\partial n}\right|_\Gamma = 0. \tag{6}$$

$\dot{m_\Gamma}$ is the mass flux per unit time across the interface. For a mono-component liquid droplet, $Y_l^\Gamma = 1$ and gradients of the species mass fraction are zero. Eq. (6) takes the form:

$$\dot{m_\Gamma} = \frac{\rho_g D \left.\frac{\partial Y_{vap}}{\partial n}\right|_\Gamma^g}{1 - Y_{vap}^\Gamma}. \tag{7}$$

The vapor mass fraction at the interface, Y_{vap}^Γ, is calculated using the Clausius-Clapeyron relation, i.e.,

$$p_{vap}^\Gamma = p_{atm} \exp\left\{\frac{h_{lg} m_{vap}}{R}\left(\frac{1}{T^\Gamma} - \frac{1}{T^B}\right)\right\}, \tag{8}$$

$$Y_{vap}^\Gamma = \frac{p_{vap}^\Gamma m_{vap}}{(p_{atm} - p_{vap}^\Gamma) m_g + p_{vap}^\Gamma m_{vap}}, \tag{9}$$

where p_{vap}^Γ is the saturated vapor pressure corresponding to the interface temperature T^Γ. T^B is the liquid boiling temperature at the ambient pressure conditions p_{atm}. R is the gas constant. m_{vap} and m_g are the molar masses of the water vapor and gas respectively.

We also assume that the material properties remain constant following a fluid particle, i.e.,

$$\frac{D\rho}{Dt} = 0; \quad \frac{D\mu}{Dt} = 0; \quad \frac{Dk}{Dt} = 0; \quad \frac{Dc_p}{Dt} = 0, \tag{10}$$

where $\frac{D}{Dt} = \frac{\partial}{\partial t} + \mathbf{u} \cdot \nabla$ is the material derivative. Indicator function $I(\mathbf{x}, t)$ tracks the liquid and the gas phases both in space and time and is defined as:

$$I(\mathbf{x}, t) = \begin{cases} 1 & \text{in droplet phase,} \\ 0 & \text{in bulk phase.} \end{cases} \tag{11}$$

The indicator function is computed using the standard procedure as described by Tryggvason et al. [15]. Then the density, viscosity, thermal conductivity and heat capacity fields are updated in each time step using the indicator function as:

$$\begin{aligned} \rho &= \rho_l I(\mathbf{x}, t) + \rho_g (1 - I(\mathbf{x}, t)); \qquad \mu = \mu_l I(\mathbf{x}, t) + \mu_g (1 - I(\mathbf{x}, t)); \\ k &= k_l I(\mathbf{x}, t) + k_g (1 - I(\mathbf{x}, t)); \qquad c_p = c_{p,l} I(\mathbf{x}, t) + c_{p,g} (1 - I(\mathbf{x}, t)). \end{aligned} \tag{12}$$

Interface location is updated at each time step by moving the interface marker points in the normal direction. The velocity of each marker point comprises of the local flow velocity and the velocity of vaporization, i.e.,

$$\frac{d\mathbf{x}_\Gamma}{dt} = u_n \mathbf{n}_\Gamma, \tag{13}$$

where

$$u_n = \frac{1}{2}(\mathbf{u}_l + \mathbf{u}_g) \cdot \mathbf{n} - \frac{\dot{q_\Gamma}}{2h_{lg}}\left(\frac{1}{\rho_l} + \frac{1}{\rho_g}\right). \tag{14}$$

3 Results and Discussion

3.1 Temperature Based Model

3.1.1 1D Stefan Problem

One-dimensional Stefan problem is a well-known test case to validate the phase change model [2, 5, 3, 13, 17]. In this case, a vertical interface separates liquid and vapor phases. The vapor is on the left side of interface and liquid is on the right side. When the temperature of the left wall of domain is increased, heat diffuses towards the interface and evaporates the liquid near the interface. As a result the interface moves towards right pushing the liquid away. The boundary condition on the right wall allows the liquid to freely leave the domain. The vapor remains stationary during this process. Therefore the heat is transferred from the left wall to the interface just by diffusion. The following form of energy equation is solved in the vapor phase only with specified boundary conditions

$$\frac{\partial T}{\partial t} = \alpha_g \frac{\partial^2 T}{\partial x^2} \qquad 0 \leq x \leq x_\Gamma(t), \tag{15}$$

$$T(x=0,t) = T_w \qquad T(x=x_\Gamma(t),t) = T_{sat}\,. \tag{16}$$

T is the temperature, α_g is the thermal diffusivity of the vapor phase and $x_\Gamma(t)$ is the interface location at time t. The analytical solution for the interface location at any time t can be expressed as

$$x_\Gamma(t) = 2\beta\sqrt{\alpha_g t}\,, \tag{17}$$

where β is the solution of the transcendental equation

$$\beta \exp(\beta^2)\,\mathrm{erf}(\beta) = \frac{c_{p,g}(T_w - T_{sat})}{h_{lg}\sqrt{\pi}}\,. \tag{18}$$

The analytical value of temperature at any point x in the vapor domain and at any time instant t is given by the expression

$$T_g(x,t) = T_w + \left(\frac{T_{sat} - T_w}{\mathrm{erf}(\beta)}\right)\mathrm{erf}\left(\frac{x}{2\sqrt{\alpha_g t}}\right). \tag{19}$$

We performed numerical simulations on a 1×1 domain. Results are presented for density ratio $\gamma = \rho_l/\rho_g = 20$. The initial interface location is set as $x_\Gamma = 0.1$, which corresponds to initial time $t_o(\gamma)$. The initial temperature field is specified in the vapor phase using analytical solution, Eq. (19), at initial time $t_o(\gamma)$. Numerical and analytical results of interface location are shown in Fig. 1 alongwith the grid convergence study.

3.1.2 2D Static Droplet

This test case simulates the evaporation of a 2D static planar droplet. Initial radius of droplet is 0.125 and it is placed at the center of 1×1 domain. Temperature difference between the outside and the inside of droplet is 5. This gradient causes evaporation and generates radial Stefan flow. Vapor is allowed to leave the domain freely, and a fixed temperature boundary condition is applied at the domain boundaries. The density and the viscosity ratios are specified as 10 and 14, respectively. Navier-Stokes equations are not solved for this case. 160×160 grid resolution ensures grid independent results. Fig. 2 plots the reduction in area, i.e., the squared diameter versus time. The squared diameter of the droplet varies linearly with time satisfying the d^2-law. For different Stefan numbers the time history of squared diameter variation follows the results in literature [10]

3.1.3 2D Moving Droplet

A 2D planar droplet is moving under the action of gravity, and evaporating due to temperature gradient. Eotvos (Eo) and Morton (Mo) numbers define the droplet shape evolution during motion, whereas the Stefan

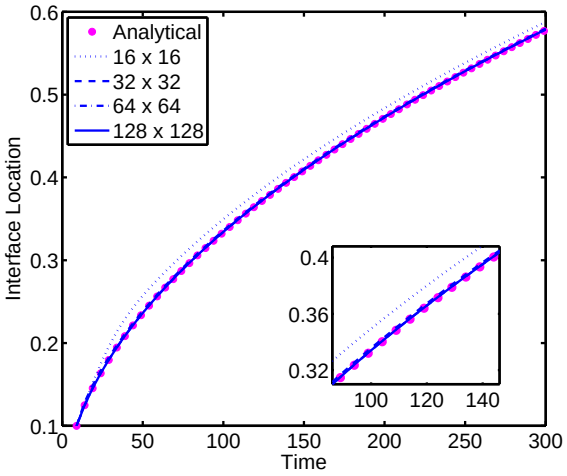

Figure 1: The evolution of the interface location compared with analytical solution for $\gamma = 20$

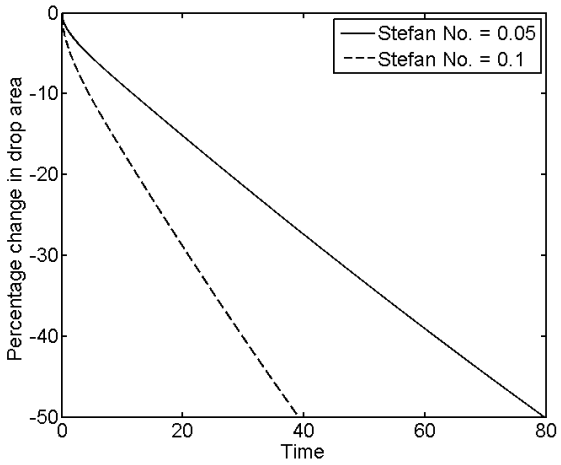

Figure 2: Time history of droplet area for two Stefan numbers.

number (St) dictates the evaporation rate. The droplet (R = 0.125) center is initially placed at (0.5,3.6) in 1×4 domain resolved by 192×768 grid. Eo = 2.34, Mo = 1.6×10^{-5}, St = 0.05, density and viscosity ratios are 10 and 14, respectively, for this test case. Wall boundary conditions are applied at the domain boundaries. A grid convergence study yields grid independent results with this resolution. Fig 3 shows the temperature contour plots at different time instants. The life time of evaporating droplet is strongly dependent on the droplet shape. As the droplet shape deviates from the spherical geometry, ratio of the surface area to the volume of droplet increases. Thus more of the droplet surface is exposed to high temperature, resulting in faster droplet evaporation.

3.2 Species Based Model

3.2.1 Evaporation Mass Flux - Validation

We consider a container partially filled with water. The remaining part of container contains dry air. The vapor gradient at the interface will drive the evaporation process.A convection-diffusion equation needs to be solved to describe the species concentration field in the gas phase. In this simplified test case, the temperature

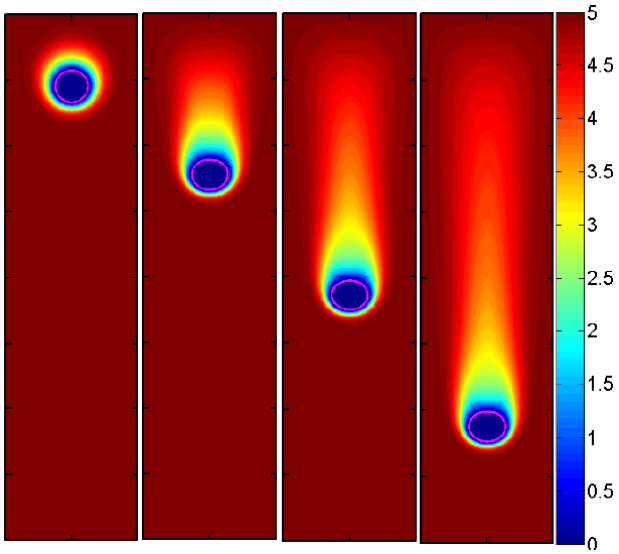

Figure 3: Temperature contour plots for a moving droplet at four time instants (time difference in each frame = 0.5).

of liquid is assumed to be constant. The air far from the interface, at the end of container, is assumed to be dry so vapor concentration is zero there. Also it is assumed that the evaporation does not reduce the quantity of water and the water level stays fixed in the container. The evaporated mass is replenished exactly and continuously. Furthermore, the surrounding gas is assumed to be insoluble in water so there is no net transport of surrounding gas in the container. At steady state condition, the evaporation mass flux per unit time at the interface, $\dot{m}_v$, is given by [11]

$$\dot{m}_v = \frac{\rho_g D}{L} \ln(1 + B), \tag{20}$$

where B is the mass number given as

$$B = \frac{Y^{\Gamma}_{vap} - Y^{L}_{vap}}{1 - Y^{\Gamma}_{vap}}. \tag{21}$$

Numerical and analytical results of non dimensional evaporation mass flux $\dot{m}_v / \frac{\rho_g D}{L}$ are plotted against mass transfer number as shown in fig. 4. It is clear that the numerical results approach the analytical profile as we refine the grid.

3.2.2 Wet/Dry Bulb Temperature - Validation

The computational setup consists of a liquid droplet of initial diameter $d_o = 0.25$ mm held stationary at the center of a 1×1 mm domain. Initially, the temperature (dry bulb temperature) is same throughout the domain and the phase change occurs due to the species gradient at the interface resulting in a low temperature/heat sink at the interface until a steady state temperature condition is attained at the interface, called the wet bulb temperature. This wet bulb temperature is a function of the dry bulb temperature (DBT) and the relative humidity (RH) in the air. A number of runs are performed for various combinations of dry bulb temperatures and relative humidities. The numerical reults of wet bulb temperatures agree very well with the psychrometric chart values as shown in fig. 5

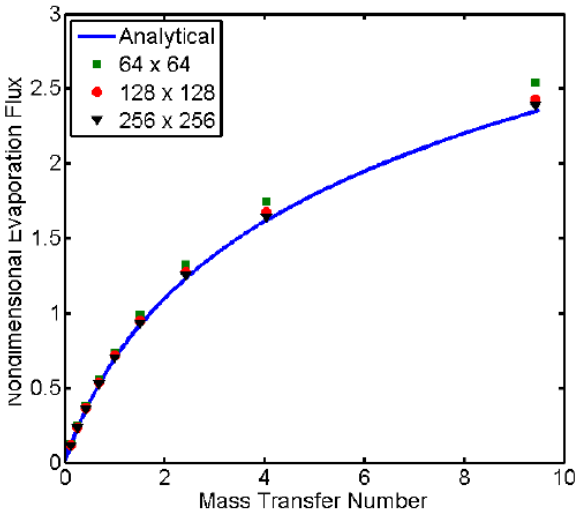

Figure 4: Comparison of analytical and numerical results for non-dimensional evaporation mass flux.

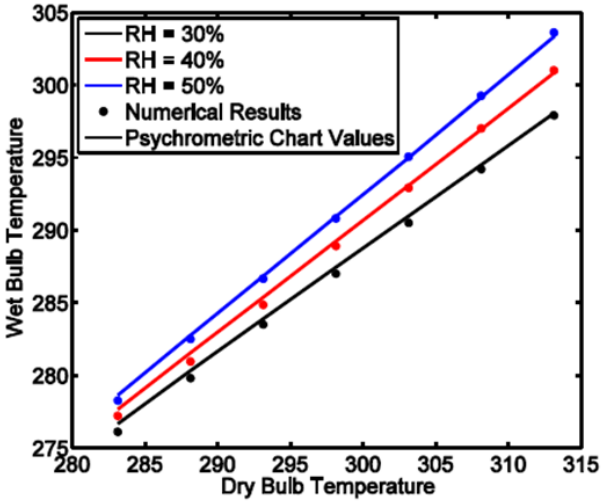

Figure 5: Numerical values of wet bulb temperatures compared with the psychrometric chart values for various combinations of dry bulb temperatures and relative humidities, grid = 128 × 128.

3.2.3 2D Moving Droplet - Global Mass Conservation

We consider a droplet that evaporates and moves due to gravity $\boldsymbol{g}$, and also deforms during the journey. Initial diameter, d_o, is 0.25 mm. The domain size is 1 × 4 mm. The droplet is initially placed with its center at (0.5,3.6) mm and starts from rest. Temperature is initialized as 353 K in the whole domain. Domain boundaries are set as walls, whereas Dirichlet boundary conditions are specified for temperature and vapor mass fraction at walls as $T_g = 353$ K and $Y_{vap} = 0$, respectively. Global mass conservation results are presented in Fig. 6. It is observed that the global mass conservation error reduces as the grid is refined. The order of accuracy is greater than one for this deformed droplet evaporation case as shown in fig. 7 which shows the ability of our method to handle deformed interfaces.

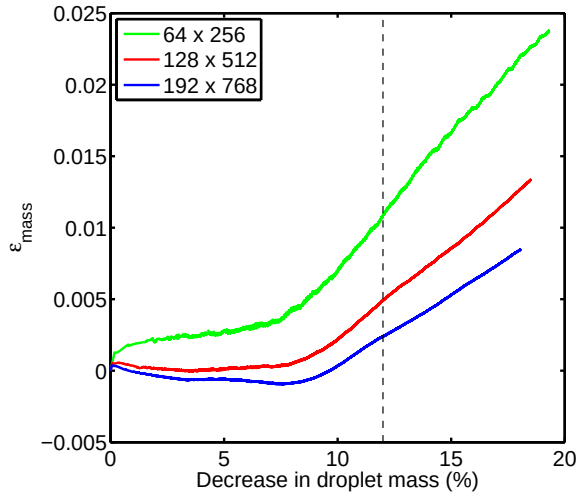

Figure 6: Global mass conservation error for a moving deforming evaporating droplet at various grid resolutions, The relevant nondimensional parameters are $Eo = 5$, $Mo = 5 \times 10^{-4}$, $Sc = 0.707$, $\gamma = 5$ and $\zeta = 1.216$

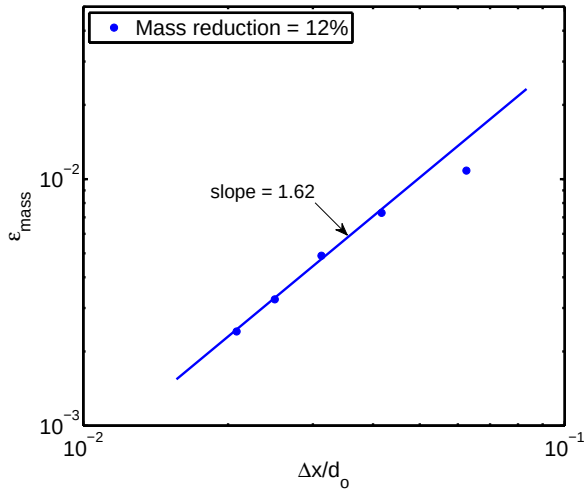

Figure 7: The global mass error versus the non-dimensional grid size after 12% loss in the droplet mass, The relevant nondimensional parameters are $Eo = 5$, $Mo = 5 \times 10^{-4}$, $Sc = 0.707$, $\gamma = 5$ and $\zeta = 1.216$

4 Conclusions and Future Work

A front-tracking method is developed to simulate the liquid vapor phase change process. Both temperature and species gradient based models are studied. Governing equations are solved in the whole domain formulation on fixed grid. Results are presented first for the temperature gradient based phase change model. Standard benchmark test cases i.e., Stefan problem and d^2-law are performed to validate our implementation. Life time of droplet is strongly dependant on the droplet shape; and increases rapidly as droplet deviates from the spherical geometry. For the species based model, evaporation mass flux and the dry/wet bulb temperature validation cases are performed which ensures the performance of the phase change and thermal solvers. For a stringent case of moving, deforming and evaporating droplet, we performed global mass conservation analysis. our implementation is grid convergent and mass is globally conserved.

We are in the process to integrate chemical kinetics solver with our solver to simulate real world problems including the droplet evaporation and combustion during spray combustion.

References

[1] A. Esmaeeli and G. Tryggvason, “Computations of Explosive Boiling in Microgravity", *J. Sci. Comput.*, **19**, 163 (2003).

[2] A. Esmaeeli and G. Tryggvason, “Computations of Film Boiling. Part I: Numerical Method", *Int. J. Heat Mass Transfer*, **47**, 5451 (2004).

[3] F. Gibou, L. Chen, D. Nguyen and S. Banerjee, “A Level Set Based Sharp Interface Method for the Multiphase Incompressible NavierâĂŞStokes Equations With Phase Change", *J. Comput. Phys.*, **222**, 536 (2007).

[4] J. Glimm, O. McBryan, R. Menikoff and D.H. Sharp, “Front Tracking Applied to Rayleigh Taylor Instability", *SIAM J. Sci. Stat. Comput.*, **7**, 230 (1986).

[5] G. Guedon, “Two-Phase Heat and Mass Transfer Modeling: Flexible Numerical Methods for Energy Engineering Analyses", Ph.D. Thesis, Politecnico Di Milano, Italy, 2013.

[6] C.W. Hirt and B.D. Nichols, “Volume of Fluid (VOF) Method for the Dynamics of Free Boundaries", *J. Comput. Phys.*, **39**, 201 (1981).

[7] D. Juric and G. Tryggvason, “A Front-Tracking Method for Dendritic Solidification", *J. Comput. Phys.*, **123**, 127 (1996).

[8] D. Juric and G. Tryggvason, “Computations of Boiling Flows", *Int. J. Multiphase Flow*, **24 (3)**, 387 (1998).

[9] S. Osher and J.A. Sethian, “Fronts Propagating with Curvature Dependent Speed: Algorithms Based on Hamilton-Jacobi Formulations", *J. Comput. Phys.*, **79**, 12 (1988).

[10] H. Safari, M.H. Rahimian and M. Krafczyk, “Extended Lattice Boltzmann Method for Numerical Simulation of Thermal Phase Change in Two-Phase Fluid Flow", *Phys. Rev. E*, **88**, 013304 (2013).

[11] H. Safari, M.H. Rahimian and M. Krafczyk, “Consistent Simulation of Droplet Evaporation Based on the Phase-Field Multiphase Lattice Boltzmann Method", *Phys. Rev. E*, **90**, 033305 (2014).

[12] J. Schlottke and B. Weigand, “Direct Numerical Simulation of Evaporating Droplets", *J. Comput. Phys.*, **227**, 5215 (2008).

[13] G. Son, V.K. Dhir, “Numerical Simulation of Film Boiling Near Critical Pressures With A Level Set Method", *J. Heat Transfer*, **120(1)**, 183 (1998).

[14] S. Tanguy, T. Menard and A. Berlemont, “A Level Set Method for Vaporizing Two-Phase Flows", *J. Comput. Phys.*, **221**, 837 (2007).

[15] G. Tryggvason, B.B. Bunner, A. Esmaeeli, D. Juric, N. Al-Rawahi, W. Tauber, J. Han, S. Nas and Y.J. Jan, “A Front-Tracking Method for the Computations of Multiphase Flow", *J. Comput. Phys.*, **169**, 708 (2001).

[16] S.O. Unverdi and G. Tryggvason, “A Front-Tracking Method for Viscous, Incompressible, Multi-Fluid Flows", *J. Comput. Phys.*, **100**, 25 (1992).

[17] S.W.J. Welch and J. Wilson, “A Volume of Fluid Based Method for Fluid Flows with Phase Change", *J. Comput. Phys.*, **160**, 662 (2000).